Journal of Electromagnetic Waves and Applications

ISSN: 0920-5071 (Print) 1569-3937 (Online) Journal homepage: http://www.tandfonline.com/loi/tewa20

Novel microstrip diplexer for ultra-wide-band (UWB) and wireless LAN (WLAN) bands

Humberto Lobato-Morales , Jim S. Sun , Alonso Corona-Chavez , Tatsuo Itoh & José Luis Olvera-Cervantes

To cite this article: Humberto Lobato-Morales , Jim S. Sun , Alonso Corona-Chavez , Tatsuo Itoh & José Luis Olvera-Cervantes (2013) Novel microstrip diplexer for ultra-wide-band (UWB) and wireless LAN (WLAN) bands, Journal of Electromagnetic Waves and Applications, 27:11, 1338-1350, DOI: 10.1080/09205071.2013.808598

To link to this article: https://doi.org/10.1080/09205071.2013.808598

Published online: 18 Jun 2013.

Journal of Electromagnetic Waves and Applications, 2013
Vol. 27, No. 11, 1338–1350, http://dx.doi.org/10.1080/09205071.2013.808598

Taylor & Francis
Taylor & Francis Group

Novel microstrip diplexer for ultra-wide-band (UWB) and wireless LAN (WLAN) bands

Humberto Lobato-Morales[a]*, Jim S. Sun[b], Alonso Corona-Chavez[a], Tatsuo Itoh[b] and José Luis Olvera-Cervantes[a]

[a]*Electronics Department, EMT Group, INAOE, Luis E. Erro No. 1, Puebla 72840, Mexico;*
[b]*Electrical Engineering, UCLA, University of California, Los Angeles 90024, USA*

(*Received 5 March 2013; accepted 22 May 2013*)

A new microstrip diplexer for ultra-wide-band (UWB) and wireless LAN (WLAN) bands is presented in this paper. The proposed structure integrates a multipole directional filter operating at WLAN band coupled to a UWB filter. The prototype is capable of processing the whole UWB region (from 3.1 to 10.6 GHz) with the WLAN band notch in one channel, and the passband WLAN band in other channel with a good selectivity due to the presence of transmission zeros at both sides of the WLAN band. The proposed diplexer is simple to fabricate, as it is designed using planar microstrip technology, and presents compact dimensions, making use of a low number of elements. Moreover, it presents the capacity of processing a narrow band (WLAN with 8% bandwidth) with a wide band (UWB). Simulated and measured results are presented with good agreement and the diplexer presents a good performance up to 15 GHz.

1. Introduction

The ultra-wide-band (UWB) signals cover a very wide region of spectrum from 3.1 to 10.6 GHz.[1–4] For such systems, multiband operation is often required, where multiplexers play an essential role. With communication systems desired to have both capabilities, such as UWB and wireless LAN (WLAN), multiplexing of their signals becomes a key issue; however, it becomes difficult for such a structure to divide or combine a very wide-band protocol, such as UWB, along with a narrow-band one as WLAN.

Due to the large fractional bandwidth requirements (110%), it is difficult to realize multiplexers covering the whole UWB in one channel along with a narrow-band channel as WLAN. In the available literature, multiplexers are not able to cover the entire UWB at a single-output channel.[1–7]

For the design of multiplexers having the capacity of channelizing the wide bandwidth of UWB signals, manifold multiplexers are not an option because they are able to channelize only narrow-band channels. A manifold multiplexer is composed of bandpass filters coupled to a main connecting structure; the separation between the different channel filters must achieve a specific electrical length to produce the

*Corresponding author. Email: humbertolm@ieee.org

directionality in each of the output ports, but because this length is frequency-sensitive, only narrow-bandwidth channels, around 10% maximum, can be obtained.[1–3]

Manifold structures having only two output ports, where two branched filters are connected to a single node instead of using connecting lines of specific electrical length, are able to increase the channel bandwidth up to 50%.[4–7]

In [4], a microstrip multiplexer, composed by two branched dual-band filters, separates the input UWB signal into two output channels from 2.15 to 2.89 GHz and from 5.13 to 5.84 GHz at one port, and two channels from 3.22 to 4.83 GHz and 6.07 to 8.22 GHz at the other output port.

In [5], a microstrip diplexer combining two bandpass filters for Bluetooth (2.4 GHz) and a portion of UWB (from 3.3 to 4.85 GHz) is reported.

In [6], two hairpin filters split the UWB into two passbands at two different output ports, a lower band going from 3.1 to 5 GHz and a higher band going from 6 to 10 GHz.

Similarly, in [7], a microstrip diplexer based on two branched filters separate the entire UWB into lower and higher passbands at two different ports, 3.1 to 4.8 GHz and 6.4 to 10.2 GHz, respectively.

Hybrid-coupled multiplexers are able to operate with wide bandwidths and channelize more than two output ports, but their main disadvantage is their large dimensions since they require two identical filters and two identical hybrid couplers per channel [7–9]; however, the full UWB channel is not easily covered by this type of multiplexers as the whole bandwidth is limited by the bandwidth of the hybrids. A hybrid-coupled multiplexer with a total bandwidth of 50% and four output ports is reported in [9]; however, it makes use of three-stage branch-line couplers for such a bandwidth. In order to design a hybrid-coupled multiplexer covering the entire UWB, hybrids with several stages are needed paying the price of additional size and weight in the multiplexer.

On the other hand, as the multiplexing of a wide-band and a narrow-band such as WLAN is being proposed, the use of directional filters as narrow-band structures is optimum as they present lower number of components and easier design, compared with manifold and hybrid-coupled multiplexers.[5–10] Moreover, they can generate multipole responses, increasing the channel selectivity.[11–12]

By using the characteristics of a multipole directional filter, the latter is integrated to a UWB filter to form a novel microstrip diplexer with the capacity of channelizing UWB and WLAN bands. The novelty of the proposed diplexer relies on its capacity of channelizing the full UWB at one output port, and WLAN at other output port, while reported diplexers in the existing literature [1–4] are able to manage only part of the UWB region or split it into different channels.

The proposed structure consists of a four-port network based on a wide-band bandpass filter coupled to a multipole directional filter operating at WLAN; both devices integrated and optimized together as one entity, producing a very compact and effective multiplexing solution rather than cascading two different components. When the signal enters Port 1, the UWB is obtained at Port 2 with suppression of the WLAN band, which is completely recovered at Port 4. The WLAN channel shows good selectivity due to the presence of transmission zeros at the edges of the band. Port 3 remains isolated, with the possibility of cascading more directional-filter stages following a module concept for channelizing additional bands.[7,10–12]

The paper is organized as follows: Section II presents the design of the diplexer, and the experimental results are shown and discussed in Section III.

2. Diplexer design

The schematic of the proposed diplexer is shown in Figure 1. It consists of a nine-pole UWB filter and an integrated two-pole directional filter operating at the WLAN band. The UWB signal (3.1–10.6 GHz) with suppression of the WLAN is obtained between Ports 1 and 2 and the WLAN band (centered at 5.4 GHz) is directed from Port 1 to Port 4. No signal is reflected to Port 1 and Port 3 remains isolated.

2.1. UWB channel

The UWB filter, used for the diplexer design, is based on the optimum-distributed high-pass filter, which consists of shunt stubs of electrical length θ_s separated by connecting lines of electrical length $\theta_c = 2\theta_s$, at the lower cutoff frequency f_1. The order of the filter is $2n-1$, n being the number of shunt stubs.[13,14]

A bandpass filter with five shunt-stubs, as shown in Figure 2, producing a nine-pole response, is designed for the UWB region. The used substrate is Rogers RT/Duroid 5880 with relative permittivity $\varepsilon_r = 2.2$, and height $h = 0.787$ mm. The lower cut-off frequency f_1 is set as 3.1 GHz and the upper cutoff frequency f_2 is located at 10.6 GHz according to the UWB specifications.[1–4] From [14], the stub length θ_s is obtained using

$$\left(\frac{\pi}{\theta_s} - 1\right) f_1 = f_2. \tag{1}$$

The calculated θ_s and θ_c values are 40.73° and 81.46°, respectively. As shown in Figure 2, Z_1 to Z_5 denote impedances of the shunt stubs and Z_{12} to Z_{45} are impedances of the connecting lines; Z_0 is the characteristic impedance, which is stated as 50 Ω. Based on the optimum-distributed highpass filter-table design in [14], impedances of each stub and connecting line for the proposed UWB filter are calculated and tabulated in Table 1.

The structure is simulated using [17], and an optimization process is carried out by slightly varying the filter dimensions. The final UWB filter geometry is shown in Figure 3(a) and its frequency response is plotted in Figure 3(b).

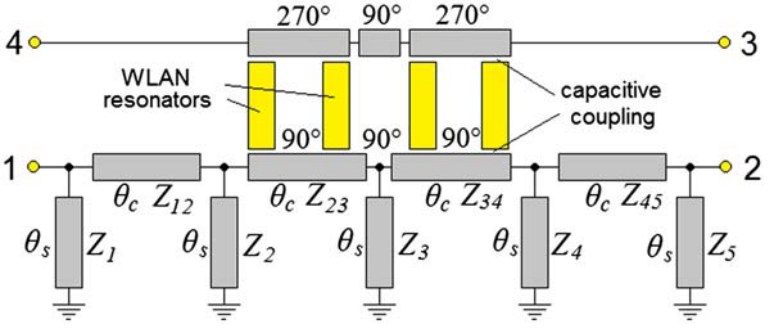

Figure 1. Schematic circuit of the proposed diplexer.

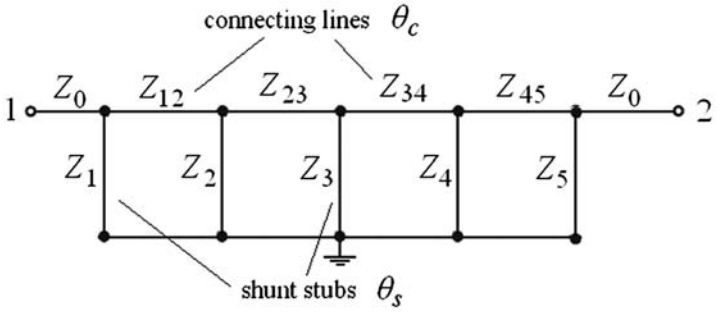

Figure 2. Schematic circuit of an optimum-distributed highpass filter [11].

Table 1. Impedances of the UWB filter shunt stubs and connecting lines.

Shunt stubs	Connecting lines
$Z_1 = Z_5 = 81.6\,\Omega$ $Z_2 = Z_4 = 54.8\,\Omega$ $Z_3 = 50\,\Omega$	$Z_{12} = Z_{45} = 51.1\,\Omega$ $Z_{23} = Z_{34} = 53.2\,\Omega$

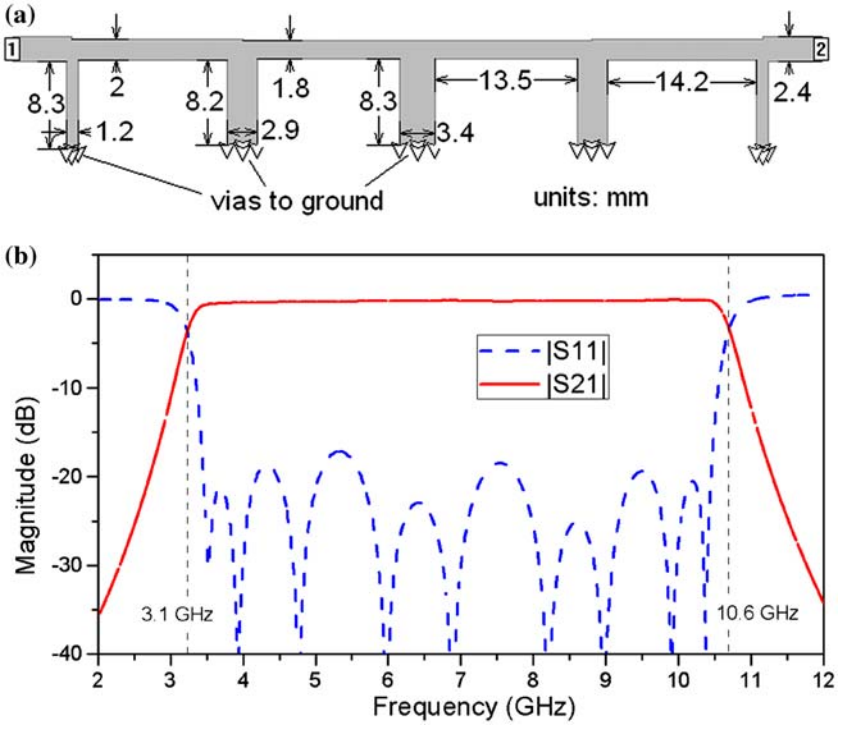

Figure 3. UWB filter (a) geometry and (b) frequency response.

2.2. WLAN channel

For the WLAN channel, a multipole directional filter operating at 5.4 GHz is designed and coupled to the main line of the UWB filter, as shown in Figure 1.

A directional filter is a four-port device having a narrow bandpass response from Ports 1 to 4, and its complementary bandstop between Ports 1 and 2; no energy is reflected to Port 1 and Port 3 remains isolated.[10–12] A multipole directional filter is able to generate narrow-bandwidth channels with good selectivity due to the presence of transmission zeros at the passband edges.[11,12]

For the WLAN channel, a two-pole directional filter operating at 5.4 GHz with 8% bandwidth is designed. The structure is composed by two stages connected by 90° lines that act as immitance inverters,[11,12] as illustrated in Figure 4. Each stage is composed of two identical resonators coupled to transmission lines of different electrical length (90° and 270°) to produce the directionality of the signal.[10–12] The operation principle of the directional filter is further analyzed in [10–12].

At the frequency region of operation, a bandstop response is obtained between Ports 1 and 2, and the complementary bandpass is directed from Ports 1 to 4; thus, the directional filter design is based on the bandstop filter approximation, which in turn is based on the reactance slope parameter x_i of each stage [11,14]

$$x_i = Z_0 \frac{1}{g_{n+1,} g_i \Omega_c \mathrm{FBW}}, \tag{2}$$

$$i = 1 \text{ to } n,\ g_0 = 1,$$

where g_i and Ω_c are the element values and cut-off of the lowpass prototype, respectively [14]; FBW is the fractional bandwidth and n is the order of the filter. The parameter x_i is related to the frequency response of a single stage by its notch 3-dB bandwidth Δf_{3dB} [14] as

$$\frac{x_i}{Z_0} = \frac{f_0}{2\Delta f_{3dB}}. \tag{3}$$

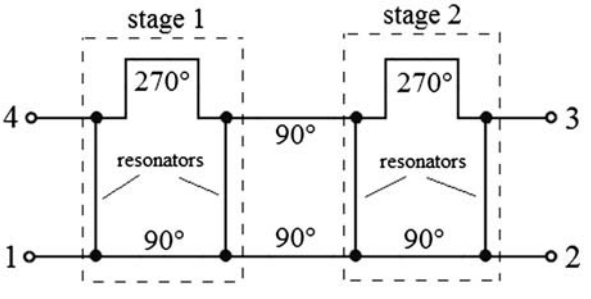

Figure 4. Schematic of the two-pole WLAN directional filter.

Table 2. Lowpass filter parameters for the design of the directional filter.

$g_0 = g_3$	$g_1 = g_2$	x_1/Z_0	x_2/Z_0	FBW
1	1.4142	8.8	8.8	0.08

Table 2 tabulates the g_i and the normalized x_i/Z_0 values for the directional filter design.[11,12] The proposed design is based on a two-pole Butterworth bandstop filter, and the lowpass g_i parameters are taken directly from [14]

As the directional filter is coupled to the UWB filter to form the diplexer, slow-wave resonators [14,16] are used since its fundamental resonance f_{s1} and first spurious f_{s2} can be adjusted at specific frequencies, producing no interference along the high-frequency region of the UWB. The resonators are designed as open microstrip lines with folded capacitive patches at both ends generating a slow-wave effect, which in turn produce the spurious frequency to separate from the fundamental resonance. The slow-wave effect in resonators is detailed in [16]. Figure 5 shows the geometry of the resonator, its simulated frequency response, and current distribution; the fundamental mode (f_{s1}) is at 5.4 GHz, and the second mode (f_{s2}) appears at 16.7 GHz, well outside the UWB region.

Stage 1 (Figure 4) is designed over the Rogers RT/Duroid 5880 substrate with height $h = 0.787$ mm. The coupling of the resonators to the transmission lines (90° and 270°) is capacitive by means of interdigital fingers for easy bandwidth control. An increase in number and length of fingers generates stronger coupling [17], consequently, the bandwidth is increased and the reactance slope parameter x_i is decreased according to (3). The reader is referred to [17] for details in capacitances using interdigital fingers.

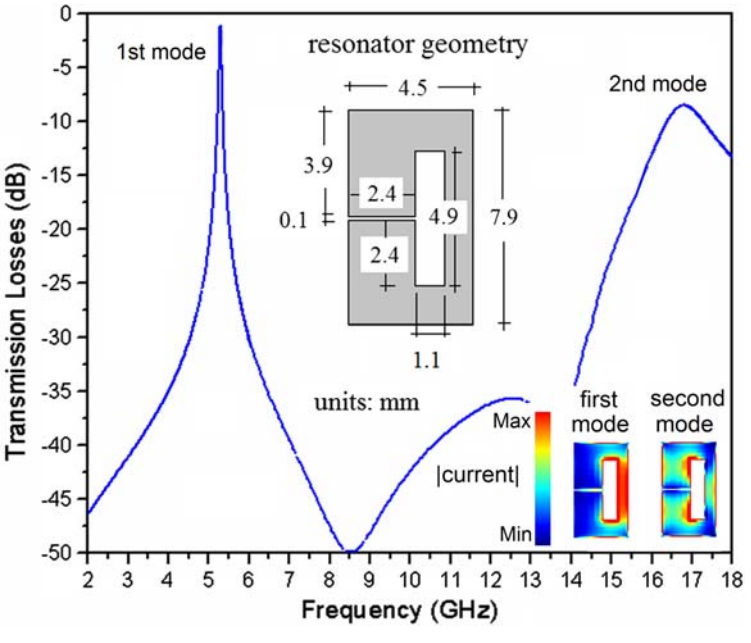

Figure 5. Geometry of the slow-wave resonator, its frequency response and current distribution.

In simulations [15], the length of the connecting lines between the resonators is optimized to obtain maximum transmission in S_{41} at the operating frequency. The longest line (270°) has been meandered for miniaturization. A parametric analysis of x_i is performed in simulations by varying the length of 15 interdigital fingers between the resonator and the connecting lines; each finger is 0.2 mm wide with a gap of 0.1 mm between them, which are the minimum achievable dimensions for fabrication using conventional photolithography. Figure 6 plots the normalized x_i value (x_i/Z_0) (3) for different length of fingers.

From Figure 6, it can be seen that interdigital fingers with length of 0.9 mm satisfy the calculated x_i value stated in Table 2. Figure 7 shows the geometry of a single stage and its frequency response.

From Figure 7(b), it can be observed that there are total transmission for S_{41} at the operating frequency 5.4 GHz. S_{21} corresponds to the complementary notch response, having a Δf_{3dB} that goes from 5.23 to 5.53 GHz, producing the desired x_1 value. Return losses S_{11} and isolation S_{31} are below −22 dB, having negligible influence with S_{21} and S_{41}.

To complete the two-pole directional filter, Stage 2 is designed identical to Stage 1 due to the symmetry of the design, and they are cascaded by means of 90° lines (immitance inverters), as shown in Figure 4. In simulations [15], the length of the immitance inverters is optimized to obtain maximum transmission for S_{41} at the operating band. Figure 8 shows the final geometry of the WLAN directional filter and its frequency response.

As it can be seen from Figure 8, although the design is based on a Butterworth filter response, two transmission zeros appear at the edges of the bandpass response (S_{41}) at 4.98 and 5.83 GHz. This can be explained by the generation of small ripples along S_{21} outside the WLAN operating region, producing zeros in S_{41}; the lines connecting the resonators and both stages are frequency-sensitive and they approximate 90° and 270°

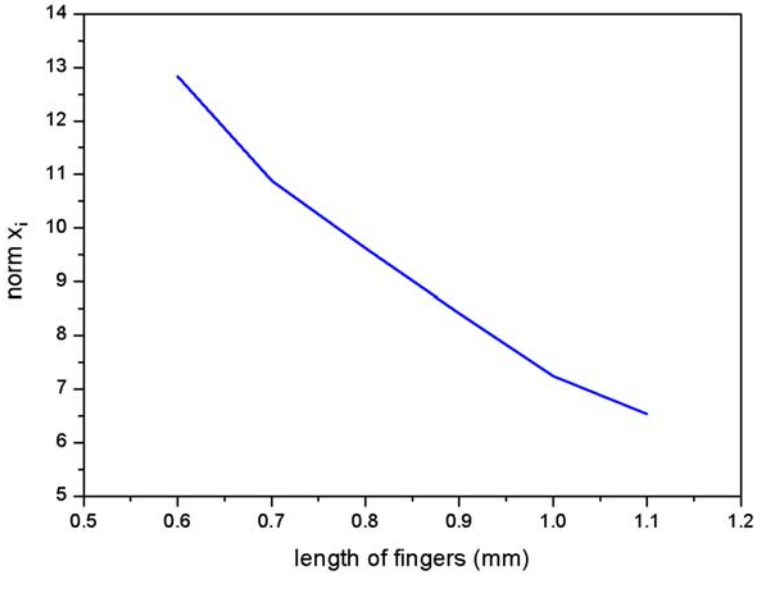

Figure 6. Normalized x_i value for different interdigital fingers length.

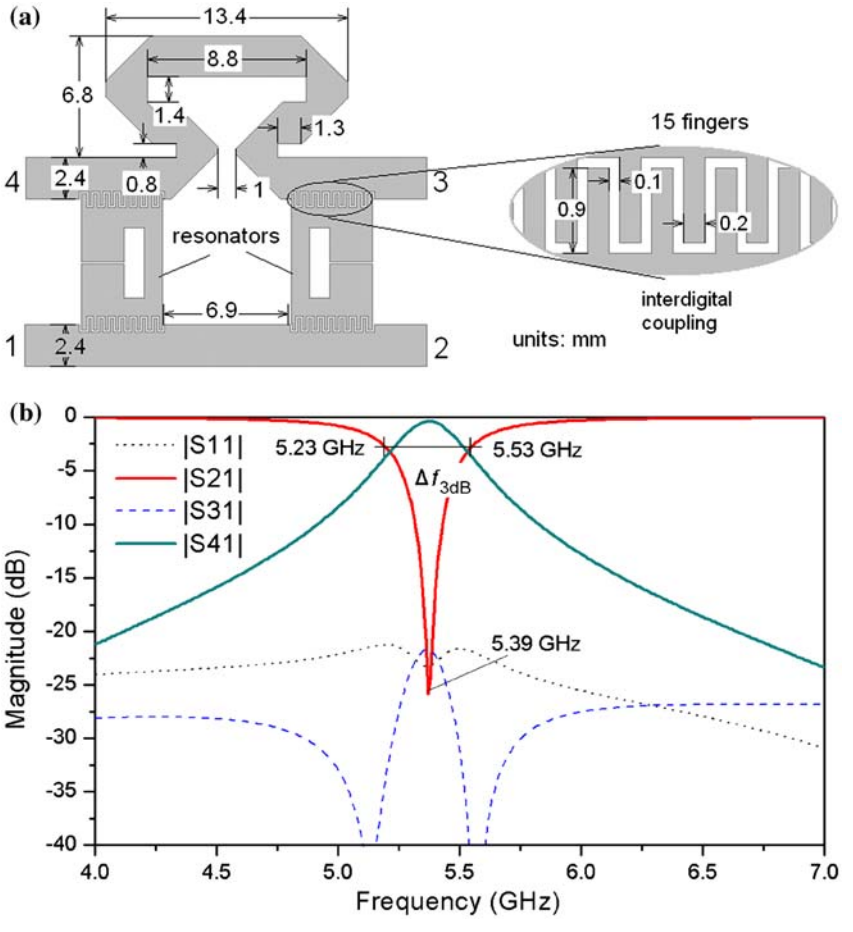

Figure 7. Single stage directional filter (a) geometry and (b) its frequency response.

only over a limited range generating standing waves outside the operating band.[10,12] However, the generation of zeros in S_{41} significantly improves the selectivity of the WLAN channel. To support this fact, simulations were carried out using ideal connecting lines (nonfrequency-sensitive lines) and the correspondent frequency response is also plotted in Figure 8(b), showing the absence of the transmission zeros, as expected.

2.3. Proposed diplexer

To form the diplexer geometry, the WLAN directional filter is coupled to the UWB filter (as shown in Figure 1); the lower line of the directional filter is replaced by the main line of the UWB filter. Although the structure is composed of the simple combination of both structures, it requires an extra optimization process in simulations.[17] The initial diplexer geometry is shown in Figure 9(a), and it is simulated with lossless materials.

For the UWB structure, the inclusion of the coupling interdigital fingers along its connecting lines causes an increase level of return losses S_{11} along the UWB region, as

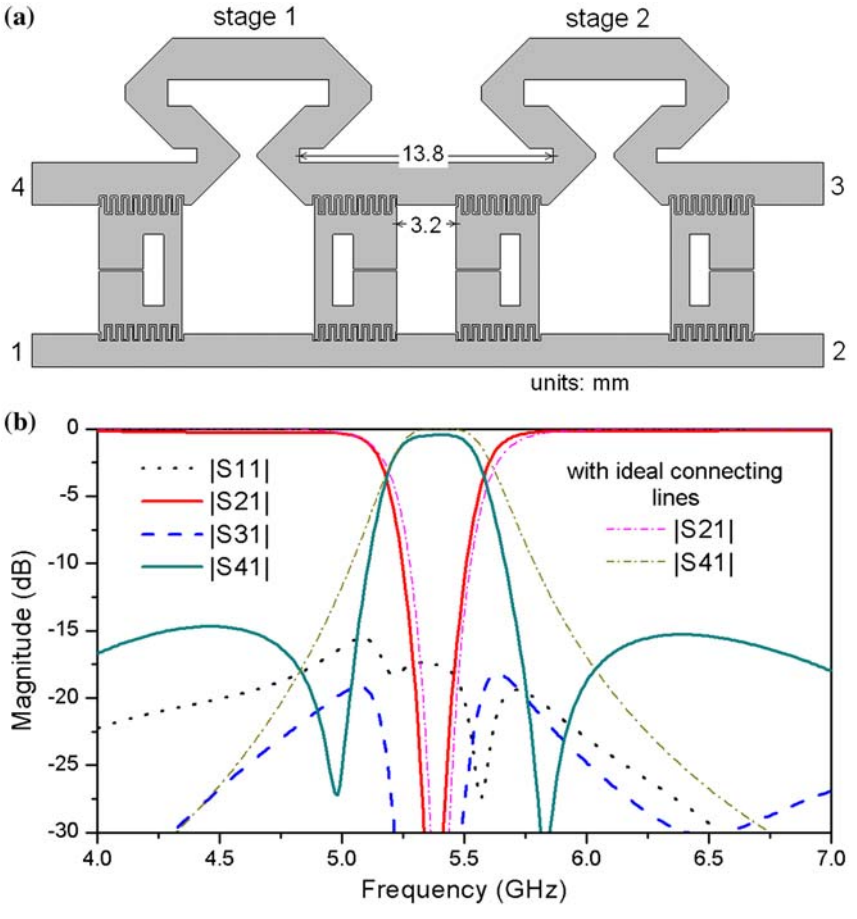

Figure 8. Two-pole directional filter (a) geometry and (b) frequency response.

can be seen in Figure 9; a first lobe at −7.4 dB at 3.35 GHz can be observed. For the S_{21} curve, a ripple of −1.3 dB is generated at 3.4 GHz. In the optimization process, this can be overcome by slightly varying the distance between shunt stubs 2 and 3, and 3 and 4 simultaneously, as it is a symmetrical structure; from the initial distance value 13.5 mm Figure 3(a), the optimized distance becomes 12.4 mm.

Within the WLAN frequency region, the highest variation due to the coupling of both the structures is also reflected in an increase level of return losses S_{11} [Figure 9(b)]. A peak of −5.8 dB at 5.15 GHz can be observed. This is due to the phase difference between the initial transmission line (immitance inverter in the directional filter) and that of the UWB filter between resonators 2 and 3 [see Figure 9(b)] in the coupling of both structures (directional filter and UWB filter). The main difference in phase is produced by the presence of the center shunt stub (with impedance Z_3 in Table 1). Also, the S_{41} curve within the WLAN region presents poor symmetry. By varying the distance between resonators 2 and 3 from 3.2 to 4.2 mm, this can be significantly improved. Length of the shunt stubs is not modified in the optimization process. The final diplexer geometry is shown in Figure 10. The lines connected to Ports 3 and 4 have been bent

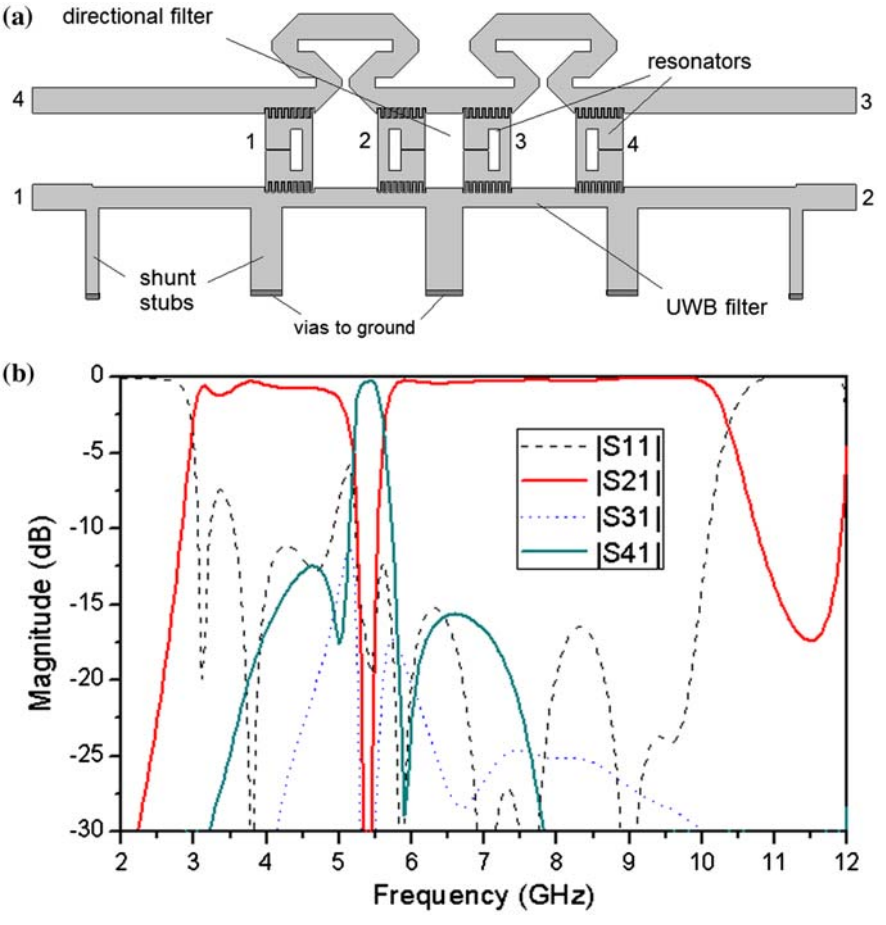

Figure 9. Proposed diplexer without optimization: (a) geometry and (b) simulatedresponse.

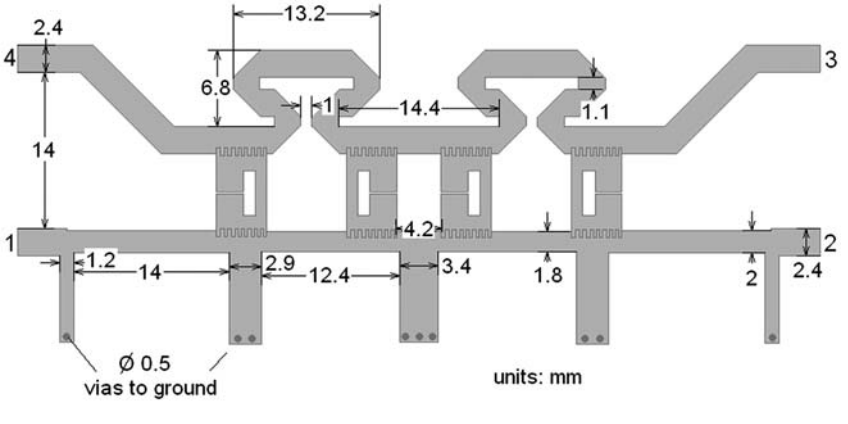

Figure 10. Final geometry of the proposed diplexer.

45° away from Ports 1 and 2 for the inclusion of the connectors in the fabricated structure.

3. Experimental results

The proposed structure is fabricated using the Rogers RT/Duroid 5880 substrate by using a photolithographic process. Overall dimensions of the diplexer are 72 mm length by 30 mm width. Figure 11 shows a photograph of the fabricated structure. The simulated [17] (including conductor, dielectric, and radiation losses) and measured responses are plotted in Figure 12(a) (S_{21} and S_{41}) and Figure 12(b) (S_{11}, S_{31}, S_{43} and S_{44}).

From Figure 12, it can be noticed that the simulated and measured responses are in good agreement. For the experimental results, maximum S_{21} losses are 0.7 dB for the UWB region between 3.2 and 5.2 GHz, and 1.8 dB for the region between 5.6 and 10.5 GHz. The measured 3 dB bandwidth for S_{21} goes from 3.1 to 5.14 GHz with a notch centered at 5.43 GHz, and continues from 5.85 to 10.7 GHz. S_{41} shows the WLAN band with 1.1 dB losses at a center frequency of 5.44 GHz with 7.2% bandwidth, from 5.26 to 5.65 GHz. Two transmission zeros at both sides of the WLAN band (5.06 and 5.875 GHz) increase its selectivity. The measured WLAN central frequency shifted 60 MHz upwards compared with simulations.

It can be observed from Figure 12(b) that the measured S_{11} and S_{31} are below -11 dB for the whole band of interest, except a small peak in S_{11} of -8.4 dB appearing at 5.25 GHz, which correspond to a peak of -11.4 dB at 5.13 GHz in simulations. The measured S_{43} response presents the WLAN band notch and is attenuated 3 dB up to 10 GHz. The measured S_{44} (equal to S_{33} due to the symmetry) remains below -10 dB for the whole UWB except around the WLAN band, where it shows two lobes of -7.3 dB at 5.1 GHz and -8.6 dB at 5.7 GHz each. As shown in Figure 12, performance of the diplexer is good up to 15 GHz.

Differences between simulated and measured responses are due to manufacturing tolerances and the inclusion of SMA connectors in the measurements.

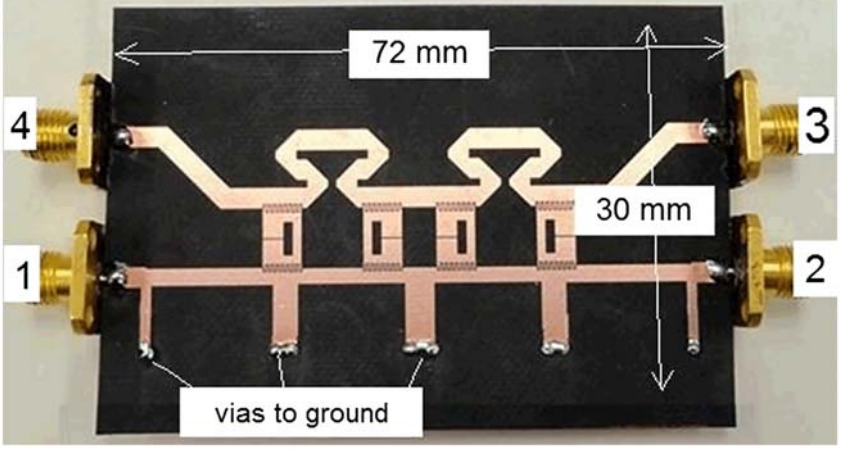

Figure 11. Photograph of the fabricated diplexer.

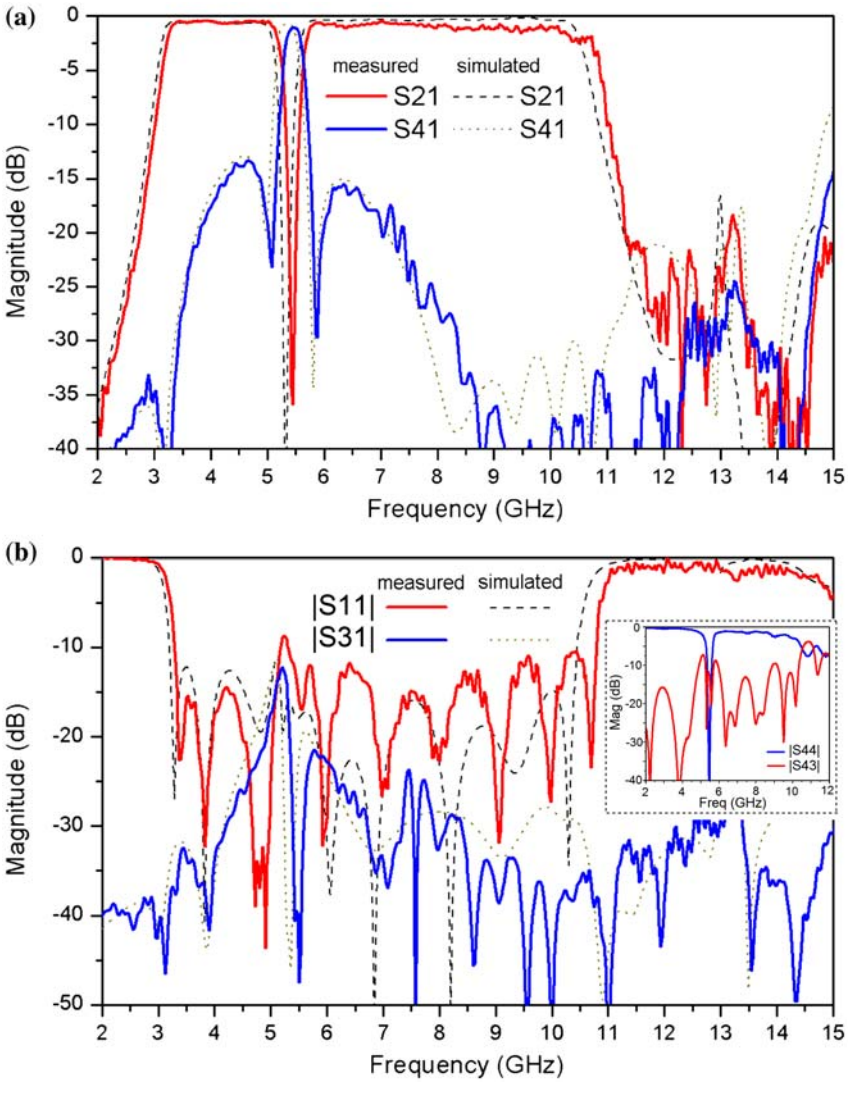

Figure 12. Simulated and measured responses of the proposed diplexer, (a) S_{21} and S_{41} and (b) S_{11} and S_{31}; measured S_{44} and S_{43} are plotted in the inset.

4. Conclusions

A new compact microstrip diplexer suitable for a very wide bandwidth along with a narrow-band channel was presented. The proposed structure makes use of two different planar circuits integrated into one single entity; an optimum distributed highpass filter and a multipole directional filter, to produce enough capacity to channelize the entire UWB and WLAN bands into two different ports. The proposed diplexer presents a good performance for both the UWB and WLAN channels. Moreover, due to the presence of transmission zeros, the WLAN channel increases its selectivity. The structure presents a compact diplexing solution, rather than using two separate devices, with an ease in its fabrication. Simulated and measured responses are in good agreement.

References

[1] Rhodes JD, Levy R. Design of general manifold multiplexers. IEEE Trans. Microw. Theory Tech. 1979;27:111–123.
[2] Luo LP, Su T, Ren ZP, Wu B. Design of helical filters manifold multiplexer using a novel equivalent circuit model. Int. Symp. Sign., Syst. Electron. 2010;1:1–4.
[3] Cameron RJ, Yu M. Design of manifold-coupled multiplexers. IEEE Microwave Mag. 2007;8:46–59.
[4] Lai MI, Jeng SK. A microstrip three-port and four-channel multiplexer for WLAN and UWB coexistence. IEEE Trans. Microw. Theory Tech. 2005;53:3244–3250.
[5] Ye CS, Su YK, Weng MH, Hung CY. A microstrip ring-like diplexer for bluetooth and UWB application. Microwave Opt. Tech. Lett. 2009;51:1518–1520.
[6] Weng MH, Hung CY, Su YK. A hairpin line diplexer for direct sequence ultra-wideband wireless communications. IEEE Microwave Wirel. Compon. Lett. 2007;17:519–521.
[7] Kuan H, Yang RY, Weng MH, Chen WL. A novel parallel-coupled line diplexer excited using slot-line resonators for ultra-wideband communications. Microwave Opt. Tech. Lett. 2009;51:1552–1555.
[8] Talisa SH, Janocko MA, Meier DL, Talvacchio J, Moskowitz C, Buck DC, Nye RS, Pieseski SJ, Wagner GR. High temperature superconducting space-qualified multiplexers and delay lines. IEEE Trans. Microwave Theory Tech. 1996;44:1229–1239.
[9] Kaur-Kataria T, Sun SP, Corona-Chavez A, Itoh T. New approach to hybrid multiplexer using composite right-left handed lines. IEEE Microwave Wireless Compon. Lett. 2011;21:580–582.
[10] Matthaei GL, Young L, Jones EMT. Microwave filters, impedance-matching networks, and coupling structures. Norwood (MA): Artech House; 1980.
[11] Lobato-Morales H, Corona-Chávez A, Olvera-Cervantes JL, Murthy DVB. Multi-pole microstrip directional filters for multiplexing applications. International Conference on Electronics, Communications and Computers; 2011 Mar; Puebla, Mexico. p. 344–349.
[12] Lobato-Morales H, Corona-Chavez A, Itoh T, Olvera-Cervantes JL. Dual-band multi-pole directional filter for microwave multiplexing applications. Microwave Wireless Compon. Lett. 2011;21:643–645.
[13] Levy R. A new class of distributed prototype filters with applications to mixed lumped/distributed component design. IEEE Microwave Theory Tech. 1970;18:1064–1071.
[14] Hong JS, Lancaster MJ. Microstrip filters for RF/microwave applications. New York (NY): Wiley; 2001.
[15] Sonnet ® EM Full-Wave Simulator, v. 13.
[16] Hong JS, Lancaster MJ. Theory and experiment of novel microstrip slow-wave open-loop resonator filters. IEEE Trans. Microwave Theory Tech. 1997;45:2358–2365.
[17] Bahl I. Lumped elements for RF and microwave circuits. Norwood (MA): Artech House; 2003.